Proceedings of the 47th International School and Conference on the Physics of Semiconductors "Jaszowiec 2018"

Excitons in Asymmetric Nanostructures: Confinement Regime

M. Gawełczyk[a,b,*]

[a]Department of Theoretical Physics, Faculty of Fundamental Problems of Technology, Wrocław University of Science and Technology, 50-370 Wrocław, Poland

[b]Department of Experimental Physics, Faculty of Fundamental Problems of Technology, Wrocław University of Science and Technology, 50-370 Wrocław, Poland

Quantum confinement of electrons and holes in semiconductor nanostructures results in quantization of their energy levels with level spacing generally decreasing with the confinement length. The relation between these splittings and the energy of the electron–hole Coulomb interaction may serve as a measure of exciton confinement regime. We consider theoretically strongly in-plane asymmetric nanostructures, like InAs/AlGaInAs elongated quantum dots. Based on optical properties, we find a possible indication of coexistence of different confinement regimes for the two bright exciton states that couple to light polarized along the two nonequivalent axes distinguished by the structural asymmetry. Exciton lifetimes and their distinct dependences on energy derived here for the two confinement regimes are in good agreement with those of recently measured double exponential photoluminescence decays. Additionally, for highly elongated dots, one of the states exhibits properties typical for the weak confinement regime, which may have a significant impact on spin relaxation processes.

DOI: 10.12693/APhysPolA.134.930

PACS/topics: 78.67.Hc, 73.21.La, 78.47.D–, 71.35.Lk

1. Introduction

The impact of the quantum confinement strength, defined by the width and depth of potential-energy well for carriers, on properties of correlated electron–hole pairs (excitons) was the subject of intensive theoretical research [1–3]. This led to formulation of the general classification into three confinement regimes (CRs) for excitons: strong, intermediate, and weak. This division is related to the relation between the confinement energy and the electron–hole Coulomb interaction energy. The measure of the former is the single-particle energy-level spacing, for the two lowest-energy states referred to as the s–p splitting $\Delta_{sp}^{(e/h)}$, where the superscript stands for electrons/holes. These splittings are strongly dependent on the characteristic length of quantum confinement, which in the case of semiconductor nanostructures is simply defined by their size. The other factor, the energy of the Coulomb attraction between the electron and the hole trapped together in the nanostructure volume, Δ_C, is less dependent on the confinement length. Therefore, with varying nanostructure size a transition from the strong, $\Delta_{sp}^{(e/h)} \gg \Delta_C$, through intermediate, $\Delta_{sp}^{(h)} < \Delta_C < \Delta_{sp}^{(e)}$, to the weak CR, $\Delta_{sp}^{(e/h)} \ll \Delta_C$, is realized.

Various CRs are characterized by distinct exciton optical properties. In the case of strong CR, mixing of single-particle states by Coulomb interaction is negligible and the exciton ground state is composed almost only of electron and hole ground states. In contrast, the weaker the confinement, the bigger the admixture of higher-energy single-particle states. Radiative recombination of such a superposition is then enhanced and its rate follows a dependence on the transition energy (dispersion) different from that met in strong CR.

Here, we investigate nanostructures strongly elongated in one of the in-plane directions, which may be exemplified by an application-relevant family of self-assembled InAs/AlGaInAs quantum dots (QDs), so-called quantum dashes [4]. We focus on conditions of exciton confinement resulting from such a geometry and, within a very simple harmonic confinement model, we find that they cannot be assigned to a single CR.

2. Confinement asymmetry

Originally [1], strong and weak exciton CRs were defined for spherically symmetric QDs in terms of the relation between the dot radius and the bulk exciton Bohr radius, a_B, while the intermediate CR was introduced for the case of high ratio of effective masses. This is directly related to the definition stated above in terms of energy, not only for spherical, but also for common QDs with lower, approximately cylindrical symmetry, if a 2D Bohr radius $a_\mathrm{2D} \approx a_\mathrm{B}/2$ is used. In such structures, the z-axis confinement defines the optical transition energy, while carrier states have the form of consecutive shells in the x–y plane very well described by the harmonic confinement model [5–7]. While for cylindrical symmetry eigenstates of radial harmonic oscillator are expected, in the case of QDs made of noncentrosymmetric semiconductors, strain-induced piezoelectric field breaks the symmetry. Then, one deals with modest splitting between states forming two axis-wise shells, which does not affect exciton properties much.

However, here we deal with significant structural asymmetry that has pronounced consequences [8, 9]. In Fig. 1, we present schematically the geometry of investi-

*e-mail: michal.gawelczyk@pwr.edu.pl

gated elongated QDs. Based on typical self-assembly of InAs/AlGaInAs quantum dashes [4], we fix the elongation (length L) along the $v \parallel [1\bar{1}0]$ axis. L may be a few times bigger than the width W (along axis $h \parallel [110]$), which is expressed in terms of the in-plane aspect ratio $\eta = L/W$. The height H is typically in the range of 1.8–3.2 nm and the cross-section geometry is fixed with $W/H \approx 6$. We assume the QD material to be 80% InAs and use material constants as in Ref. [9].

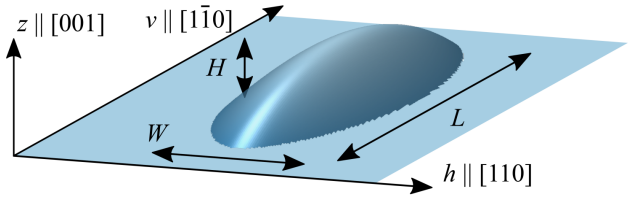

Fig. 1. A schematic view of the system with basic parameters and polarization axes defined.

3. Theoretical considerations

To qualitatively assess the properties of excitons in a highly asymmetric QD, we assume an axis-wise anisotropic harmonic confinement with electron/hole potential energy given by

$$V_{e/h}(\boldsymbol{r}) = \frac{1}{2} m_{e/h} \sum_{i=v,h,z} \left[\omega_i^{(e/h)}\right]^2 x_i^2, \tag{1}$$

where $\omega_i^{(e/h)} = \hbar/(m_{e/h} l_i^2)$, $m_{e/h}$ is the effective mass, and l_i is the characteristic confinement length in the i axis, typically a few times (N_i) smaller than the actual QD size, which corresponds to $\prod_i \mathrm{erf}(N_i/2)$ of carrier density localized within a box-like QD. Considering the real geometry of investigated QDs and recently calculated wave functions [9], we use: $l_v = L/4$, $l_h = (W/2)/3$ (division by 2 due to the triangular shape), and $l_z = H/(2\sqrt{2})$. The resulting envelope wave functions are of the product form

$$\Psi_{nm}(\boldsymbol{r}) = \psi_n(x)\psi_m(y)\psi_0(z), \tag{2}$$

where $\psi_n(x_i)$ is the n-th eigenfunction of the 1D harmonic oscillator along the axis x_i and we assume no excitations along z. Full eigenstates in the multi-band approach are then $\boldsymbol{\Psi}_{nm}(\boldsymbol{r}) = \sum_\mu \Psi_{nm}^{(\mu)}(\boldsymbol{r})\,|\mu\rangle$, where $|\mu\rangle$ are the zone-center Bloch functions [10], and μ runs over the lowest conduction, heavy- (hh) and light-hole (lh) valence bands. For simplicity, we neglect all band mixing except the opposite-spin lh admixture to the hh ground state (identical envelopes assumed). The corresponding orbital energies are

$$E_{nm}^{(\alpha)} = \hbar\omega_v^{(\alpha)}\left(n+\frac{1}{2}\right) + \hbar\omega_h^{(\alpha)}\left(m+\frac{1}{2}\right) + \frac{1}{2}\hbar\omega_z^{(\alpha)}, \tag{3}$$

for $\alpha = e, h$, which scales with the QD size as $E_{nm}^{(\alpha)} - E_0^{(\alpha)} \propto n/L^2 + m/W^2$, where the ground-state energy is $E_0^{(\alpha)} = \hbar\sum_i \omega_i^{(\alpha)}/2 \simeq \hbar\omega_z^{(\alpha)}/2$ (as $L^2, W^2 \gg H^2$). Excitations along each of the axes are equidistant in energy, with spacing $\Delta_{v/h}^{(\alpha)} = \hbar\omega_{v/h}$, proportional to $1/L^2$ and $1/W^2$, respectively. For a given aspect ratio η one has thus $\Delta_h^{(\alpha)}/\Delta_v^{(\alpha)} = \eta^2$, so we deal with a dense ladder of states with antinodes located along the v-axis sparsely interspersed by those along the h-axis.

Given the 2D exciton Bohr radius $a_{2D} \approx 14$ nm and a typical elongated QD with $W = 18$ nm and $L = 80$ nm, we may initially notice that $W/2 < a_{2D} < L/2$, so assigning a single CR based on this criterion fails. However, treating the axes separately, one finds that they would fall into different regimes. In terms of energy, for typical electron–hole Coulomb interaction $\Delta_C \simeq 15$ meV, we find for both types of carriers that $\Delta_v^{(\alpha)} < \Delta_C < \Delta_h^{(\alpha)}$ ($\Delta_v^{(e)} \approx 6$ meV, $\Delta_h^{(e)} \approx 270$ meV, $\Delta_v^{(h)} \approx 0.6$ meV, $\Delta_h^{(h)} \approx 26$ meV). This may be expected to result in considerable admixtures of states with antinodes located along the QD (and lack of the other) in the exciton ground state, which appears to be a manifestation of a "mixed" CR.

The in-plane asymmetry leads also to the hh–lh subband mixing [8, 11] with eigenstates $\boldsymbol{\Psi}_{nm}^{h,\Uparrow'/\Downarrow'}(\boldsymbol{r}) \propto \Psi_{nm}(\boldsymbol{r})(|\Uparrow / \Downarrow\rangle + \mathrm{i}\epsilon\,|\downarrow / \uparrow\rangle)$, where $\Uparrow / \Downarrow$ and $\uparrow / \downarrow$ stand for the hh ($m = \pm 3/2$) and lh ($m = \pm 1/2$) states, respectively, while $\epsilon \in \mathbb{R}_>$ may be up to a few % for highly elongated QDs [9]. This changes the nominally circular polarization of bright-exciton dipole moments into elliptical with major axes inclined towards the v axis for both states. Including the anisotropy also in the electron–hole exchange interaction [12], yields states that couple to light polarized linearly along v and h axes with unequal oscillator strengths, $f_v > f_h$ [9]. Such a difference of lifetimes of two cross-polarized photoluminescence intensities has recently been observed [13, 14] with significant difference in dispersion of the two lifetimes [9].

We propose to interpret this in terms of two coexisting CRs: strong for the state coupled to h-polarized light, and weak for the other one. As already mentioned, one expects more efficient recombination in the weak CR. Additionally, the two dispersions should also vary. In the dipole approximation, radiative lifetime is given by [15]:

$$\tau = \frac{6\pi\varepsilon_0 m_0 c^3 \hbar^2}{n e^2 f E_X^2}, \tag{4}$$

where n is the refractive index, f is the oscillator strength, E_X is the transition energy, and other symbols stand for usual constants. In the strong CR the exciton ground state is approximately given by the product of electron and hole ground states, which yields

$$f_{\mathrm{SCR}} = \frac{2}{m_0 E_X}\left|\int_V \mathrm{d}^3\boldsymbol{r}\,\boldsymbol{\Psi}_{00}^{h,\Uparrow}\boldsymbol{r}\widehat{\boldsymbol{p}}\,\boldsymbol{\Psi}_{00}^{e,\downarrow}(\boldsymbol{r})\right|^2 = \frac{\vartheta E_P}{2E_X}, \tag{5}$$

where $\widehat{\boldsymbol{p}}$ is the momentum operator, E_P is the Kane energy, and $0 \le \vartheta \le 1$ is the overlap of electron and hole envelopes. Substituted into Eq. (4), it gives a $\tau_{\mathrm{SCR}} \propto 1/E_X$ dispersion. On the other hand, one may estimate the os-

cillator strength in the weak CR starting with the 2D "bulk" case and replacing the quantum-well volume V with the electron–hole overlap (QD) volume [15], here estimated as $V_X \simeq LWH/2 = 3H^2L$,

$$f_{\rm 2D} = \frac{E_P}{2E_X}\frac{V}{\pi a_{\rm 2D}^2 H} \longrightarrow f_{\rm WCR} \propto \frac{3E_P}{2\pi a_{\rm 2D}^2}\frac{HL}{E_X}. \qquad (6)$$

For the ground state one has $E_X \simeq E_0^{(e)} + E_0^{(h)} - \Delta_C \simeq 9\hbar^2/(2\mu H^2)$, where $\mu^{-1} = m_e^{-1} + m_h^{-1}$ and we neglected $\Delta_C \ll E_0^{(e/h)}$. Inserting this into Eq. (6) and then to Eq. (4), we obtain $\tau_{\rm WCR} \propto 1/(L\sqrt{E_X})$, where L may be treated as fixed, as it has almost no impact on the transition energy.

In Fig. 2, we plot experimentally obtained radiative lifetimes taken from Ref. [9] (symbols) along with lines representing the two trends considered here (for $\epsilon = 0.05$, $\vartheta = 0.75$, and $L = 80$ nm). The agreement seems reasonable in view of the simplicity of the model we used and may serve as a partial confirmation for the presence of different CRs for the two bright exciton states. However, a further careful investigation of electron–hole interactions in such elongated QDs is needed to determine whether the two states actually differ in the amount of higher-orbital admixtures.

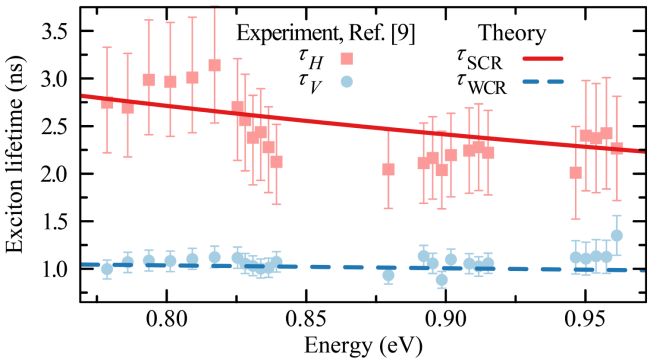

Fig. 2. Dispersion of the two unequal exciton radiative lifetimes: experimentally estimated values taken from Ref. [9] (symbols) and theoretical curves obtained using Eq. (5) (solid line) and Eq. (6) (dashed line).

4. Conclusions

We have investigated asymmetric semiconductor nanostructures focusing on the CR for excitons. Strong asymmetry leads to approximately independent sub-ladders of energy states corresponding to carrier wave-function antinodes placed along and across the axis of nanostructure elongation. Based on the approximation with an axis-wise-asymmetric harmonic confinement and recent numerical results obtained for realistic geometry of elongated QDs, we have found a coexistence of different CRs for excitons. By this we mean that level spacing of electron/hole excitations may be much higher than the energy of electron–hole Coulomb interaction in the case of one of the two orthogonal in-plane axes, and lower for the other one. Additionally, anisotropy in the electron–hole exchange interaction fixes the polarization of optical transition for the two lowest-energy bright exciton states along these two axes. Thus, one deals with excitons that couple to light polarized linearly along the two axes and behave according to the stronger or weaker CR. We have shown that recently measured lifetimes of the two states actually follow trends derived here for strong and weak CRs. Apart from consequences exhibited in optical properties, this may have a critical impact on, e.g., carrier spin relaxation in such structures. While the latter is typically suppressed in QDs, the partially weak CR means unfrozen center-of-mass motion in the v-axis, which should enable the Elliot–Yafet [16, 17] and the D'yakonov–Perel' [18] mechanisms. Indirect indication of enhanced spin relaxation in elongated QDs has recently been reported [19]. Hence, a wider study of this issue along a few topical paths is needed.

Acknowledgments

The work was supported by Grant No. 2014/14/M/ST3/00821 from the Polish National Science Centre. Calculations have been carried out using resources provided by Wrocław Centre for Networking and Supercomputing (http://wcss.pl), Grant No. 203. I would like to thank Marcin Syperek, Krzysztof Gawarecki, and Paweł Machnikowski for valuable discussions.

References

[1] Al.L. Éfros, A.L. Éfros, *Fiz. Tekh. Poluprovodn.* **5**, 2191 (1982) [*Sov. Phys. Semicond.* **16**, 772 (1982)].

[2] S.I. Pokutnyi, *Phys. Lett. A* **168**, 433 (1992).

[3] Al.L. Éfros, A.V. Rodina, *Phys. Rev. B* **47**, 10005 (1993).

[4] A. Sauerwald, T. Kümmell, G. Bacher, A. Somers, R. Schwertberger, J.P. Reithmaier, A. Forchel, *Appl. Phys. Lett.* **86**, 253112 (2005).

[5] A. Wójs, P. Hawrylak, S. Fafard, L. Jacak, *Phys. Rev. B* **54**, 5604 (1996).

[6] P. Hawrylak, G.A. Narvaez, M. Bayer, A. Forchel, *Phys. Rev. Lett.* **85**, 389 (2000).

[7] K. Teichmann, M. Wenderoth, H. Prüser, K. Pierz, H.W. Schumacher, R.G. Ulbrich, *Nano Lett.* **13**, 3571 (2013).

[8] A. Musiał, P. Kaczmarkiewicz, G. Sęk, P. Podemski, P. Machnikowski, J. Misiewicz, S. Hein, S. Höfling, A. Forchel, *Phys. Rev. B* **85**, 035314 (2012).

[9] M. Gawełczyk, M. Syperek, A. Maryński, P. Mrowiński, Ł. Dusanowski, K. Gawarecki, J. Misiewicz, A. Somers, J.P. Reithmaier, S. Höfling, G. Sęk, *Phys. Rev. B* **96**, 245425 (2017).

[10] R. Winkler, *Spin–Orbit Coupling Effects in Two-Dimensional Electron and Hole Systems*, Springer, Berlin 2003.

[11] A.V. Koudinov, I.A. Akimov, Yu.G. Kusrayev, F. Henneberger, *Phys. Rev. B* **70**, 241305 (2004).

[12] M. Bayer, G. Ortner, O. Stern, A. Kuther, A.A. Gorbunov, A. Forchel, P. Hawrylak, S. Fafard, K. Hinzer, T.L. Reinecke, S.N. Walck, J.P. Reithmaier, F. Klopf, F. Schäfer, *Phys. Rev. B* **65**, 195315 (2002).

[13] H. Tahara, Y. Ogawa, F. Minami, K. Akahane, M. Sasaki, *Phys. Rev. B* **87**, 035304 (2013).

[14] M. Syperek, Ł. Dusanowski, M. Gawełczyk, G. Sęk, A. Somers, J.P. Reithmaier, S. Höfling, J. Misiewicz, *Appl. Phys. Lett.* **109**, 193108 (2016).

[15] J. Bellessa, V. Voliotis, R. Grousson, X.L. Wang, M. Ogura, H. Matsuhata, *Phys. Rev. B* **58**, 9933 (1998).

[16] R.J. Elliott, *Phys. Rev.* **96**, 266 (1954).

[17] Y. Yafet, *Phys. Rev.* **85**, 478 (1952).

[18] M.I. D'yakonov, V.I. Perel', *Zh. Eksp. Teor. Fiz.* **60**, 1954 (1971) [*Sov. Phys. JETP* **33**, 1053 (1971)].

[19] Ł. Dusanowski, M. Gawełczyk, J. Misiewicz, S. Höfling, J.P. Reithmaier, G. Sęk, *Appl. Phys. Lett.* **11**, 043103 (2018).